

Analysis of Axially Symmetric Wire Antennas by the Use of Exact Kernel of Electric Field Integral Equation

Aleksandra J. Krneta¹, Branko M. Kolundžija¹

Abstract: The paper presents a new method for the analysis of wire antennas with axial symmetry. Truncated cones have been applied to precisely model antenna geometry, while the exact kernel of the electric field integral equation has been used for computation. Accuracy and efficiency of the method has been further increased by the use of higher order basis functions for current expansion, and by selecting integration methods based on singularity cancelation techniques for the calculation of potential and impedance integrals. The method has been applied to the analysis of a typical dipole antenna, thick dipole antenna and a coaxial line. The obtained results verify the high accuracy of the method.

Keywords: Wire antennas, Exact kernel, Electric field integral equation, Method of moments.

1 Introduction

The analysis of axially symmetric antennas has been a subject of great interest among the researchers interested in computational electromagnetics and antenna design. Accordingly, the subject has been studied intensively in the past. From the perspective of this paper, the prior work in the field can be roughly divided in two categories. The first category includes methods that use the exact kernel of the electric field integral equation to increase the accuracy of the calculations, while the modeling of antenna geometry is simplified to include cylinders [1 – 14]. The second category comprises methods where antenna geometry is more accurately modeled by applying truncated cones, but using the reduced kernel of the electric field integral equation. This modeling approach has been used in [15, 16].

Along with the methods which use the exact kernel, the potential, field and impedance integrals were calculated using integration methods based on singularity extraction technique. The extraction has been combined with

¹School of Electrical Engineering, University of Belgrade, King Alexander's Blvd 73, 11020 Belgrade, Serbia;
E-mails: krneta@etf.bg.ac.rs; kol@etf.bg.ac.rs

derivation of analytical expressions of particular parts of integrals in the form of infinite sums or elliptic integrals, as in [1 – 13]. In [14], a method based on singularity cancelation technique has been used for calculation of these integrals.

The motivation behind the work described in this paper was to further increase accuracy and efficiency of the analysis of axially symmetric wire antennas. The method described in this paper for the first time combines precise modeling of the antenna geometry by using truncated cones with the exact kernel of the electric field integral equation. For calculation of potential and impedance integrals, integration methods based on singularity cancelation technique are applied. Furthermore, the quadruple integral is reduced to a triple integral by introducing a change of variables, increasing even further the high efficiency of the method.

General information on the electric field integral equation method and specific details about modeling of the antenna, basis functions and test procedures are all presented in Section II. The final forms of impedance integrals, appearing in the system matrix, are also derived there. Section III presents the calculated results for current distribution, near and far field of a typical dipole antenna, thick dipole antenna and a coaxial cable. For the case of a typical dipole antenna the results have been compared with the results obtained using the MoM method with reduced kernel (WIPL-D program [17]). The convergence of the results as the order of current approximation increases is also considered in Section III. Finally, the conclusions are summarized in Section IV.

2 Description of the Method

Consider an axially symmetric wire structure made of a perfect conductor and driven by one or more ideal voltage generators of angular frequency ω . A symmetric wire dipole shown in Fig. 1, is a typical representative of such an antenna. It has a bi-conical feeder region and conical ends.

If a wire structure is driven by one or more generators, the surface currents are induced on its surface. The unknown distribution of the surface currents can be found by solving the electric field integral equation using the Method of Moment (MoM) [18, 19]. Once the current distribution is known, all other parameters of interest can be determined.

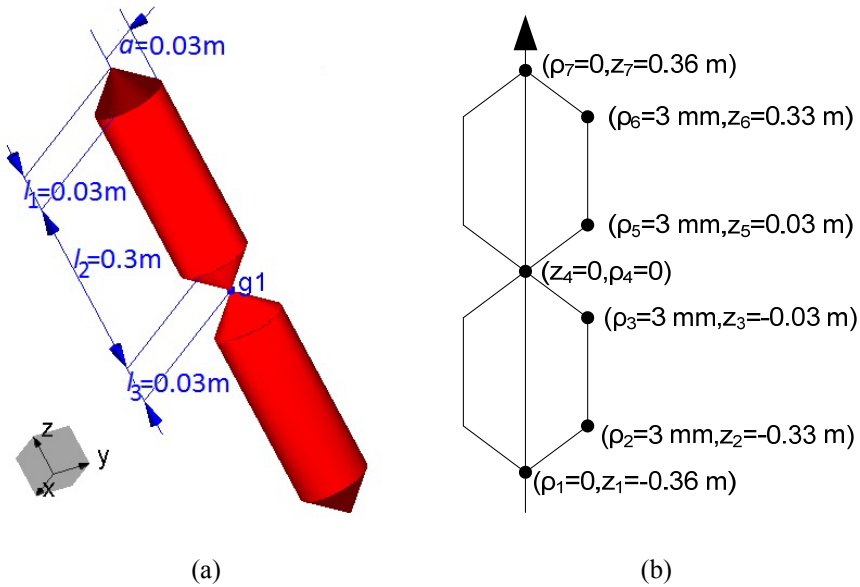


Fig. 1 – A typical example of an axially symmetric antenna – symmetric dipole with bi-conical feeder region and conical ends: (a) 3D display; (b) longitudinal section.

2.1 Integral equation

The EM field outside of the structure is uniquely defined by the known distribution of the incident field of the generator and by the boundary condition for the tangential component of the electric field on the surface of the wire structure

$$\mathbf{E}_{\text{tan}} = 0. \quad (1)$$

Outside the generator region, the electric field can be expressed as the sum of the electric field of surface currents $\mathbf{E}(\mathbf{J}_s)$ and the incident field of the driving generator \mathbf{E}_{inc}

$$\mathbf{E} = \mathbf{E}(\mathbf{J}_s) + \mathbf{E}_{\text{inc}}. \quad (2)$$

As the field vanishes inside the perfect conductors, the interior of the antenna can be replaced with vacuum. Providing that the surface of the antenna is replaced with the surface current sheet where current distribution is equal to the distribution of currents flowing on the surface of the original antenna, the electromagnetic field elsewhere would not change. Therefore, the problem can be reduced to the existence of the surface currents in vacuum, and so the electric field due to induced currents can be expressed by the integral expression

$$\mathbf{E}(\mathbf{J}_s) = -Z L(\mathbf{J}_s), \quad (3)$$

where L is the linear operator acting on the surface current \mathbf{J}_s given by

$$L(\mathbf{J}_s) = j\beta \int_{S'} \left[\mathbf{J}_s(\mathbf{r}')g(R) + \frac{1}{\beta^2} \nabla' \cdot \mathbf{J}_s(\mathbf{r}') \nabla g(R) \right] dS', \quad (4)$$

$$g(R) = \frac{e^{-j\beta R}}{4\pi R}, \quad R = |\mathbf{r} - \mathbf{r}'|, \quad (5)$$

where \mathbf{r}' is the position vector of the source point, \mathbf{r} is the position vector of the field point, $\beta = \omega\sqrt{\epsilon\mu}$ is the phase coefficient, $Z = \sqrt{\mu_0/\epsilon_0}$ is the intrinsic (wave) impedance of vacuum, and $g(R)$ is the Green's function.

After replacing (3) into (1) we obtain

$$Z L(\mathbf{J}_s)_{\text{tan}} = (\mathbf{E}_{\text{inc}})_{\text{tan}}, \quad (6)$$

which represents the electric field integral equation (EFIE). This is the typical equation which is solved by the MoM. The first step in the use of the MoM is geometrical modeling of the problem.

2.2 Geometrical Modeling of the Problem

In this paper wire structure is divided into n segments in the form of truncated cones. Every segment can be uniquely defined via the center coordinate \mathbf{r}_c , displacement vector \mathbf{r}_s , the mean radius a_c and the increment of the radius Δa . The relationship between these parameters and the coordinates of the beginning and the end point are

$$\mathbf{r}_c = \frac{\mathbf{r}_1 + \mathbf{r}_2}{2}, \quad \mathbf{r}_s = \frac{\mathbf{r}_2 - \mathbf{r}_1}{2}, \quad (7)$$

$$a_c = \frac{a_1 + a_2}{2}, \quad \Delta a = \frac{a_2 - a_1}{2}, \quad (8)$$

where \mathbf{r}_1 is the position vector of the beginning of the segment beginning, a_1 is the radius of the truncated cone at that point, and \mathbf{r}_2 and a_2 are, respectively the position vector and the radius at the segment end.

Let us introduce a local s -axis which can be set along the axis of the wire so that point $s = -1$ coincides with the beginning of the segment, and $s = 1$ coincides with the end of the same segment. Let us also introduce a local p -axis which circulates around the surface of the segment so that upon the increment from $p = -1$ to $p = 1$ a whole circle is described around the surface of the segment. In that case every point on the segment can be uniquely expressed in terms of local p - and s -coordinates as

$$\mathbf{r} = \mathbf{r}_c + \mathbf{r}_s s + a(s) \hat{\mathbf{i}}_p(p), \quad (9)$$

$$a(s) = a_c + \Delta a s, \quad (10)$$

$$\mathbf{i}_p(p) = \cos(p\pi)\mathbf{i}_x + \sin(p\pi)\mathbf{i}_y, \quad (11)$$

where $a(s)$ is the radius at the observed height of the segment and $\mathbf{i}_p(p)$ is the unit radius vector.

It is useful to define unitary vectors \mathbf{a}_p and \mathbf{a}_s and corresponding unit vectors \mathbf{i}_p and \mathbf{i}_s as

$$\mathbf{a}_p = \frac{d\mathbf{r}}{dp} = a(s)(-\pi \sin(p\pi)\mathbf{i}_x + \pi \cos(p\pi)\mathbf{i}_y), \quad (12)$$

$$\mathbf{a}_s = \frac{d\mathbf{r}}{ds} = \mathbf{r}_s + \Delta a \mathbf{i}_p, \quad (13)$$

$$\mathbf{i}_p = \frac{\mathbf{a}_p}{a_p}, \quad \mathbf{i}_s = \frac{\mathbf{a}_s}{a_s}, \quad (14)$$

where $a_p = |\mathbf{a}_p| = a_{(s)}\pi$ and $a_s = |\mathbf{a}_s|$ are the intensities of unitary vectors \mathbf{a}_p and \mathbf{a}_s . Therefore, \mathbf{a}_p and \mathbf{a}_s represent tangents to the surface of the segment in the direction for which s - and p -coordinate is constant, respectively.

2.3 Basis functions

The unknown surface current at the k^{th} segment is represented as the sum of basis functions

$$\mathbf{J}_s = \sum_{k,i} x_{ki} \mathbf{F}_{ki}, \quad (15)$$

where \mathbf{F}_{ki} is the i^{th} basis function at the k^{th} segment, and x_{ki} are the unknown coefficients that need to be determined. Surface current \mathbf{J}_s can have only the component in the direction of the unit vector \mathbf{i}_s . Accordingly, the basis functions used in this paper are given by

$$\mathbf{F}_{ki} = \frac{f_i \mathbf{a}_{sk}}{2|\mathbf{a}_{pk} \times \mathbf{a}_{sk}|}, \quad (16)$$

where f_i are scalar higher order basis functions of s -coordinate given with

$$f_i(s) = \begin{cases} \frac{1-s}{2}, & i=0 \\ \frac{1+s}{2}, & i=1 \\ s^i - s^{i-2}, & i \geq 2 \end{cases}. \quad (17)$$

Basis function f_1 at the k^{th} segment and basis function f_0 at the $k+1^{\text{st}}$ segment are coupled in a unique function, called the doublet, which automatically satisfies the current continuity equation at the junction of those segments. Basis functions f_i for $i \geq 2$ have zero values at both ends of the segment and they are called the singlets.

2.4 Test procedure: General form of matrix elements

By expressing the surface current with finite number of unknown coefficients as in (15), EFIE cannot be satisfied at every point on the surface of the wire structure. Consequently, the test procedure determines the way in which the EFIE is satisfied. It is defined by the inner product of the test function and the boundary condition (in this case the EFIE from (6)) and in most cases it is realized in a form of an integral. In this work the Galerkin test procedure is chosen, which tests the boundary condition with each basis function inside of the domain in which it exists. In this manner, the equations from which the unknown coefficients can be determined have the form

$$\int_{S_l} \mathbf{F}_{lj} \cdot \mathbf{E}(\mathbf{J}_s) dS_l = \int_{S_l} \mathbf{F}_{lj} \cdot \mathbf{E}_{\text{inc}} dS_l, \quad (18)$$

where \mathbf{F}_{lj} is the j^{th} basis function at the l^{th} segment. After expressing \mathbf{J}_s in (3) using (15) we obtain

$$\mathbf{E}(\mathbf{J}_s) = -Z \sum_{k,i} x_{ki} L(\mathbf{F}_{ki}). \quad (19)$$

After replacing (19) into (18) the system of linear equations is obtained in the form

$$\sum_{k,i} x_{ki} Z_{ljki} = G_{lj}, \quad (20)$$

where Z_{ljki} are the impedance integrals and G_{lj} are the elements of the column vector of constant terms (which will be analyzed in detail in the next chapter). The impedance integrals Z_{ljki} represent the elements of the system matrix and they are given by

$$\begin{aligned} Z_{ljki} = j\beta Z \int_{S_l} \int_{S_k} & \left[\mathbf{F}_{lj}(s_l) \cdot \mathbf{F}_{ki}(s_k) g(R) \right. \\ & \left. + \frac{1}{\beta^2} \nabla_k \cdot \mathbf{F}_{ki}(s_k) \nabla g(R) \cdot \mathbf{F}_{lj}(s_l) \right] dS_k dS_l. \end{aligned} \quad (21)$$

In (21) the local coordinate s_k corresponds to the source point on the surface of the k^{th} segment, and s_l corresponds to the field point on the surface of the l^{th} segment. Similarly to the case studied in [19], (21) can be transformed using partial integration to take the following form:

$$Z_{ljki} = j\beta Z \int_{S_j} \int_{S_k} \left[\mathbf{F}_{lj}(s_l) \cdot \mathbf{F}_{ki}(s_k) - \frac{1}{\beta^2} \nabla_l \cdot \mathbf{F}_{lj}(s_l) \nabla_k \cdot \mathbf{F}_{ki}(s_k) \right] g(R) dS_k dS_l. \quad (22)$$

In this way, the field integral is reduced to the potential integral, because unlike in (21), it is no longer needed to differentiate the Green's function. After using (16) in (22), calculating the divergence of basis functions and expressing each surface element as $dS = |\mathbf{a}_p \times \mathbf{a}_s| dp ds$, the impedance integral becomes

$$Z_{ljki} = \frac{j\beta Z}{4} \int_{p_l=-1}^1 \int_{s_l=-1}^1 \int_{p_k=-1}^1 \int_{s_k=-1}^1 \left[f_j(s_l) f_i(s_k) \mathbf{a}_{s_l} \cdot \mathbf{a}_{s_k} - \frac{1}{\beta^2} \frac{df_j(s_l)}{ds_l} \frac{df_i(s_k)}{ds_k} \right] g(R) ds_k dp_k ds_l dp_l. \quad (23)$$

Having in mind that scalar product $\mathbf{a}_{s_l} \cdot \mathbf{a}_{s_k}$ and distance R depend only on the difference of the parametric coordinates p_l and p_k , we can conclude that the whole integrand depends on the difference, not on a coordinate alone. For this reason, the quadruple integral can be simplified using the change of variables $p_k = p_l - p$. After the replacement (23) is reduced to

$$Z_{ljki} = \frac{j\beta Z}{4} \int_{p_l=-1}^1 \int_{s_l=-1}^1 \int_{p=p_l-1}^{p_l+1} \int_{s_k=-1}^1 \left[f_j(s_l) f_i(s_k) \mathbf{a}_{s_l} \cdot \mathbf{a}_{s_k} - \frac{1}{\beta^2} \frac{df_j(s_l)}{ds_l} \frac{df_i(s_k)}{ds_k} \right] g(R) ds_k dp ds_l dp_l. \quad (24)$$

Since the p -coordinate is proportional to the angle between the source point and the field point, the integrand is periodic with respect to the p -axis with a period of 2. For this reason, the boundaries for the integration by the p -coordinate can be translated to the range from -1 to 1, without affecting the value of the integral. The integral does not depend any more on the coordinate p_l , and the fourth integration (by the p_l -coordinate) can be performed independently from other three. The result of the integration is 2. The final form of the impedance integral is given with the expression

$$Z_{ljki} = \frac{j\beta Z}{2} \int_{s_l=-1}^1 \int_{p=-1}^1 \int_{s_k=-1}^1 \left[f_j(s_l) f_i(s_k) \mathbf{a}_{s_l} \cdot \mathbf{a}_{s_k} - \frac{1}{\beta^2} \frac{df_j(s_l)}{ds_l} \frac{df_i(s_k)}{ds_k} \right] g(R) ds_k dp ds_l. \quad (25)$$

Since the derivatives of the polynomial basis functions are also polynomial functions, the impedance integral can be expressed as the linear combination of two types of integrals

$$P_{ji} = \int_{s_l} \int_p \int_{s_k} s_l^j s_k^i g(R) ds_k dp ds_l, \quad (26)$$

$$Q_{ji} = \int_{s_l} \int_p \int_{s_k} s_l^j s_k^i \cos(\pi p) g(R) ds_k dp ds_l. \quad (27)$$

Each of three integrations in the integrals (26) and (27) has quasi-singular behavior and thus, their numerical calculation requires a lot of integration points if the standard Gauss-Legendre integration rules are applied. In order to improve the efficiency, all three integrations in (26) and (27) are numerically calculated by the use of integration methods based on the singularity cancelation technique. First, the integration along the s_k -coordinate is preformed using the change of variables which has been explained in detail in [20]. Transformations used for the integration along the p - and s_k -coordinate are similar to ones considered in [14, 21, 22].

2.5 Test procedure: The general form of the vector of free terms

In (20) G_{ij} are the elements of the column vector of constant terms. The expression for G_{ij} can be deduced from (18) as

$$G_{ij} = \int_{S_l} \mathbf{F}_{ij}(s_l) \cdot \mathbf{E}_{\text{inc}}(s_l) dS_l, \quad (28)$$

In this paper, the excitation is modeled in a form of one or more point generators of voltage U . Therefore, it is taken that the width of the generator d is approaching zero. For this reason the incident field, which exists inside the generator, can be described as

$$E_{\text{inc}} = U \delta(l - l_0), \quad (29)$$

where l_0 is the position of the observed generator, and δ is the delta function. After expressing the scalar basis functions f_j in (16) with (17) and after the substitution of (29) in (28), expression for an element G_{ij} becomes

$$G_{ij} = \int_{l_s} f_j U \delta(l - l_0) dl_s, \quad (30)$$

where l_s is the path across the surface of the segment for the fixed angle (that is for $p_l = \text{const.}$). The expression (30) has the value of $G_{ij} = U$ if the generator is placed at the junction of two segments where f_j is the corresponding doublet. Otherwise the integral in (30) has zero value $G_{ij} = 0$.

3 Results

The first example which is analyzed is a symmetric dipole antenna shown in Fig. 1. It is driven by an ideal point generator of frequency $f = 300$ MHz and voltage $U = 1$ V. Dimensions and diameter of the dipole are also shown in Fig. 1. The order of current approximation used for conical segments is $n = 1$, and for cylindrical segments is $n = 2$.

In Fig. 2 comparison of the results for the current distribution is shown in the s -coordinate system for the second segment. In Fig. 3 the radiation pattern is shown in the plane which contains the axis of the dipole.

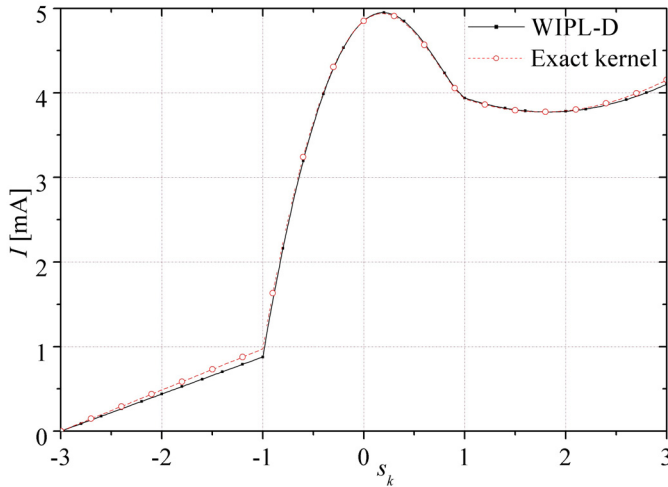


Fig. 2 – Current distribution of the dipole along the s -coordinate in the reference system of the second segment compared with the results of WIPL-D software.

From Figs. 2 and 3 it can be seen that the results of the presented method match very well with the simulation results in WIPL-D. The small deviation is most likely due to different kernels used for the electric field integral equation when setting the problem.

The next example is a symmetric dipole antenna from Fig. 1, but with changed dimensions $l_1 = 0.15$ m, $l_2 = 0.15\sqrt{2}$ m, $l_3 = 0.15$ m and with radius $a = 0.15$ m. From the dimensions we can conclude that it is a thick dipole antenna with the overall arm length of $l = 0.512$ m. In Fig. 4 the comparison of current distribution along the dipole arm is given for several orders n of current approximation and in Fig. 5 the mean value of the relative error of current intensity versus the approximation order is shown in logarithmic scale.

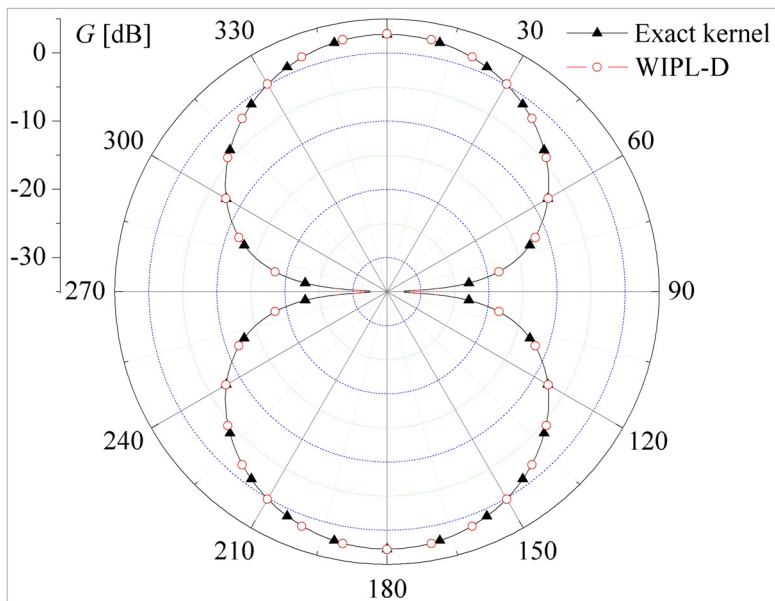


Fig. 3 – Results for the radiation pattern of the dipole compared with the results of WIPL-D software.

From Figs. 4 and 5 it is seen that very accurate results with relative error less than 1.4 % are already obtained with order $n = 3$. Also, it can be concluded that results converge until the order of $n = 23$, when the relative error is around 0.1 %. Thus, the range of polynomial order which can be used for the analysis is very large, which additionally confirms the precision of the method.

The near field of the thick dipole is shown in Fig. 6. Since the field in the perfect conductor (PEC) is theoretically zero, the calculated field level inside the structure can be used as a measure of solution quality. For this example the electric field inside the dipole is around 0.5 V/m which is negligibly small compared to the maximal value of the electric field in the diagram. These results overall confirm that this method can be used for precise analysis of thick wire antennas with axial symmetry.

The model of the coaxial cable is shown in the inset of Fig. 7. The length of the cable without the conical ends is $h = 0.5\lambda$ at the reference frequency $f = 300$ MHz. Radius of the inner conductor is $a = \lambda/400$, and the ratio of the outer and inner conductor is $b/a = 2.3$, thus the coaxial cable has the characteristic impedance of $Z_c = 50 \Omega$. The conical regions form the angle θ at both ends of the cable. The line is driven by two generators (one at the input and one at the output).

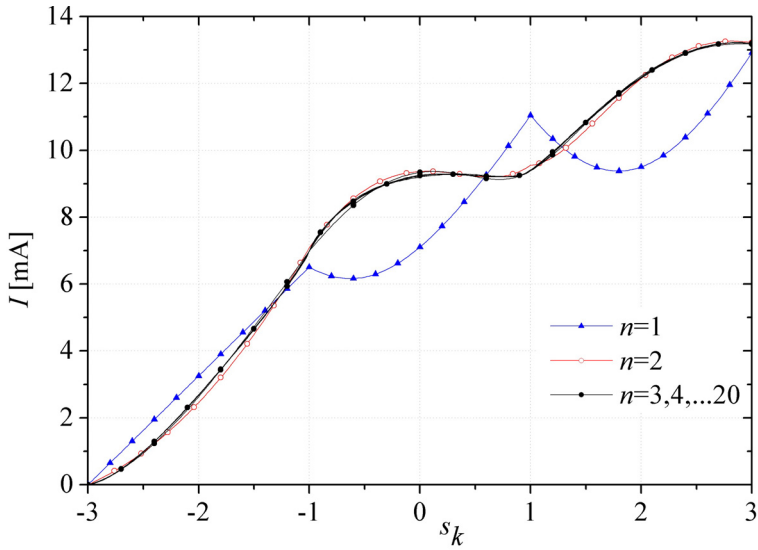


Fig. 4 – Comparison of current intensity of the thick dipole antenna for different orders of current approximation.

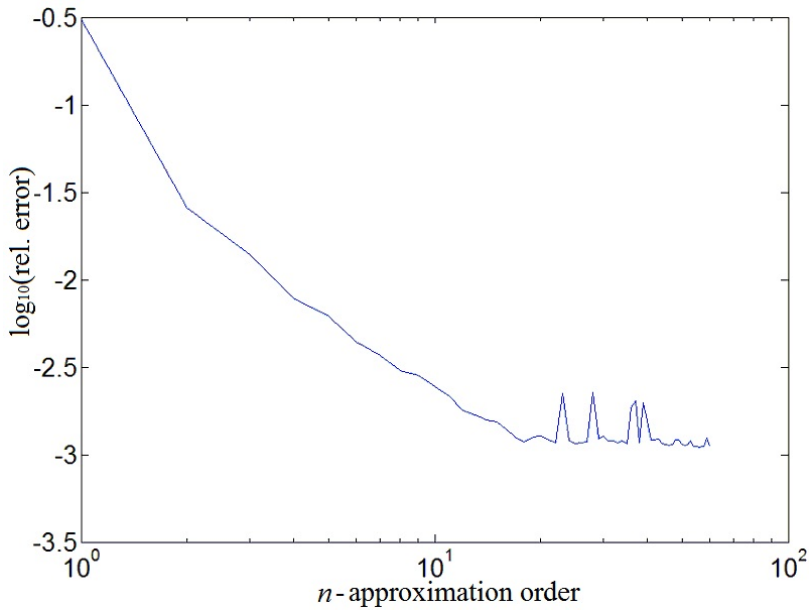


Fig. 5 – The relative error in logarithmic ratio versus the order of current approximation for the thick dipole antenna.

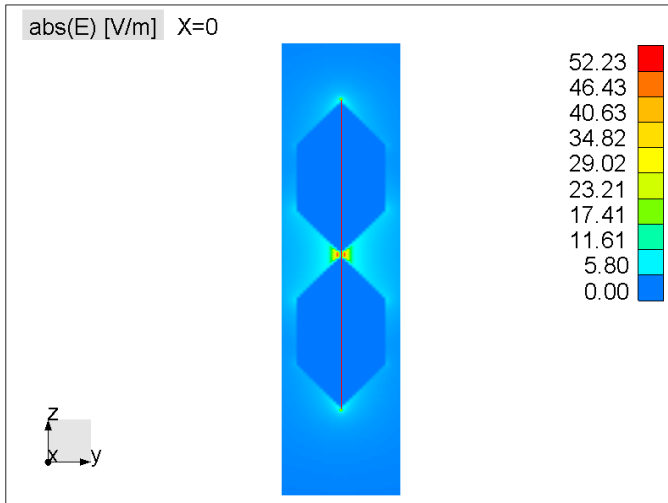


Fig. 6 – The near field along the longitudinal section of the thick dipole antenna.

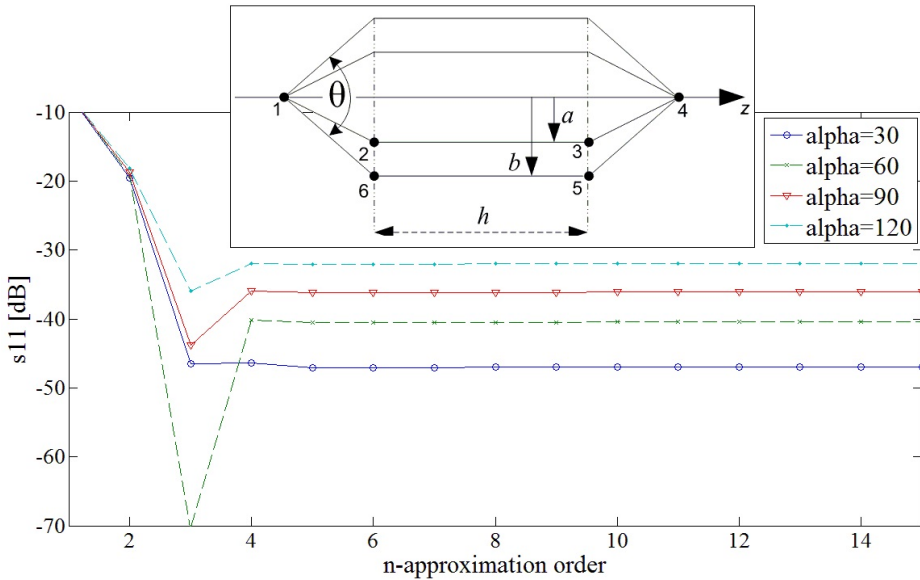


Fig. 7 – The model of the coaxial cable and s_{11} parameter (in dB) versus the order of the current approximation.

Parameter s_{11} versus the current approximation order is presented in Fig. 7. As expected, the value of s_{11} parameter is very small for all the presented values of angle θ . It is seen that when decreasing the angle θ the s_{11} parameter

decreases as well. The results also show that when increasing the current approximation order the value of s_{11} parameter converges. Accordingly, for the presented results the best match is obtained for the case of $\theta = 30^\circ$ when s_{11} converges to the value of -47 dB. Therefore, these results confirm that the method can be used for efficient analysis of axially-symmetric wire structures of arbitrary shape.

4 Conclusion

In the paper a new method is presented for the analysis of axially symmetric wire antennas which consolidates several principles in order to achieve higher accuracy. The unknown current distribution is determined by solving the electric field integral equation using the MoM method. The exact kernel of the electric field integral equation is applied. For precise geometry modeling of the structure truncated cones are used. The surface current is approximated with higher order basis functions. Final expressions of the impedance integrals, which represent the elements of the system matrix, are also derived. In these expressions figure fourfold integrals which are reduced to threefold integrals by the use of change of variables. The remaining threefold integral is numerically calculated using the singularity cancellation method.

On the example of a typical dipole antenna, the agreement between the results of this method and the simulation results of WIPL-D software is shown for the current distribution and radiation pattern. The convergence of the results for the mean relative error of current intensity and for the s_{11} parameter is analyzed on the example of a thick dipole antenna and a coaxial cable. It is shown that the results converge with increasing the order of current approximation. Accordingly, high precision of the presented method is confirmed. With these results it is also shown that the method can be used for extremely efficient analysis of complex wire structures of arbitrary shape with axial symmetry.

5 Acknowledgement

The work presented here is supported in part by Serbian Ministry of Education, Science and Technical development under the grant TR-32005.

6 References

- [1] F.D.Q. Pereira, J.L.G. Tornero, D.C. Rebenague, J.P. Garcia, A.A. Melcon: Analysis of Thick-wire Antennas using a Novel and Simple Kernel Treatment, *Microwave Optical and Technology Letters*, Vol. 46, No. 4, Aug. 2005, pp. 410 – 417.
- [2] A. Heldring, J.M. Rius: Efficient Full-kernel Evaluation for Thin Wire Analysis, *Microwave Optical and Technology Letters*, Vol. 44, No. 5, March 2005, pp. 477 – 480.

- [3] A. Mohan, D.S. Weile: Accurate Modeling of the Cylindrical Wire Kernel, *Microwave Optical and Technology Letters*, Vol. 48, No. 4, April 2006, pp. 740 – 744.
- [4] P.J. Papakanellos: Assessment of a Simple Technique for the Computation of Singular Potential and Reaction Integrals Occurring in Thin-wire Antenna Analysis, *Microwave Optical and Technology Letters*, Vol. 49, No. 2, Feb. 2007, pp. 462 – 467.
- [5] U.C. Resende, M.V. Moreira, M.M. Afonso: Evaluation of Singular Integral Equation in MoM Analysis of Arbitrary Thin Wire Structures, *IEEE Transaction on Magnetics*, Vol. 50, No. 2, Feb. 2014, p. 7011204.
- [6] A.M.A. Jalloul, J.L. Young: Singularity Evaluation of the Straight-wire Mixed-potential Integral Equation in the Method of Moments Procedure, *IEEE Transaction on Antennas and Propagation*, Vol. 59, No. 1, Jan. 2011, pp. 172 – 179.
- [7] A. Mohan, D.S. Weile: Convergence Properties of Higher Order Modeling of the Cylindrical Wire Kernel, *IEEE Transaction on Antennas and Propagation*, Vol. 55, No. 5, May 2007, pp. 1318 – 1324.
- [8] D.H. Werner: A Method of Moments Approach for the Efficient and Accurate Modeling of Moderately Thick Cylindrical Wire Antennas, *IEEE Transaction on Antennas and Propagation*, Vol. 46, No. 3, March 1998, pp. 373 – 382.
- [9] S.-O. Park, C.A. Balanis: Efficient Kernel Calculation of Cylindrical Antennas, *IEEE Transaction on Antennas and Propagation*, Vol. 43, No. 11, Nov. 1995, pp. 1328 – 1331.
- [10] D.H. Werner, J.A. Huffman, P.L. Werner: Techniques for Evaluating the Uniform Current Vector Potential at the Isolated Singularity of the Cylindrical Wire Kernel, *IEEE Transaction on Antennas and Propagation*, Vol. 42, No. 11, Nov. 1994, pp. 1549 – 1553.
- [11] W.-X. Wang: The Exact Kernel for Cylindrical Antenna, *IEEE Transaction on Antennas and Propagation*, Vol. 39, No. 4, Apr. 1991, pp. 434 – 435.
- [12] C.H. Butler: Evaluation of Potential Integral at Singularity of Exact Kernel on Thin-Wire Calculations, *IEEE Transaction on Antennas and Propagation*, Vol. 23, No. 2, March 1975, 293 – 295.
- [13] L.W. Pearson: A Separation of the Logarithmic Singularity in the Exact Kernel of the Cylindrical Antenna Integral Equation, *IEEE Transaction on Antennas and Propagation*, Vol. 23, No. 2, March 1975, pp. 256 – 258.
- [14] D.R. Wilton, N.J. Champagne: Evaluation and Integration of the Thin Wire Kernel, *IEEE Transaction on Antennas and Propagation*, Vol. 54, No. 4, April 2006, pp. 1200 – 1206.
- [15] A.R. Djordjevic, B.D. Popovic, M.B. Dragovic: Analysis of Electrically Thick Antennas of Revolution, 3rd International Conference on Antennas and Propagation, Norwich, UK, 12-15 April 1983, pp. 390 – 394.
- [16] B.M. Kolundžija, B.D. Popovic: Entire-domain Galerkin Method for Analysis of Generalized Wire Antennas and Scatterers, *IEE Proceedings H - Microwaves, Antennas and Propagation*, Vol. 139, No. 1, Feb. 1992, pp. 17 – 24.
- [17] WIPL-D Pro Version 11, WIPL-D d.o.o., Belgrade, Serbia, 2015. Available at: www.wipl-d.com.
- [18] R.F. Harrington: *Time-Harmonic Electromagnetic Fields*, McGraw-Hill, New York, NY, USA, 1961.
- [19] B.M. Kolundžija A.R. Djordjevic: *Electromagnetic Modeling of Composite Metallic and Dielectric Structures*, Artech House, Norwood, MA, USA, 2002.
- [20] A.J. Krneta, B.M. Kolundžija: Comparison of Two Methods for Calculation of Integral of Potentials in Analysis of Thin Wire Structures, *ETRAN Conference, Vrnjačka Banja, 02-05 Jun 2014, AP1.3. 1 – 6*. (In Serbian).

- [21] A.G. Polimeridis, J.R. Mosig: Evaluation of Weakly Singular Integrals Via Generalized Cartesian Product Rules Based on the Double Exponential Formula, IEEE Transaction on Antennas and Propagation, Vol. 58, No. 6, June 2010, pp. 1980 – 1988.
- [22] A.G. Polimeridis, I.D. Koufogiannis, M. Mattes, J.R. Mosig: Considerations on Double Exponential-based Cubatures for the Computation of Weakly Singular Galerkin Inner Products, IEEE Transaction on Antennas and Propagation, Vol. 60, No. 5, May 2012, pp. 2579 – 2582.